ADVANCES IN ATMOSPHERIC SCIENCES, VOL. 40, DECEMBER 2023, 2183–2194

• **Original Paper** •

Impact of the Shrinkage of Arctic Sea Ice on Eurasian Snow Cover Changes in 1979–2021※

Qian YANG[1], Shichang KANG[*1,2], Haipeng YU[3], and Yaoxian YANG[3]

[1]*State Key Laboratory of Cryospheric Science*, *Northwest Institute of Eco-Environment and Resources*, *Chinese Academy of Sciences*, *Lanzhou* 730000, *China*

[2]*University of Chinese Academy of Sciences*, *Beijing* 100049, *China*

[3]*Key Laboratory of Land Surface Process and Climate Change in Cold and Arid Regions*, *Northwest Institute of Eco-Environment and Resources*, *Chinese Academy of Sciences*, *Lanzhou* 730000, *China*

(Received 23 September 2022; revised 30 January 2023; accepted 20 February 2023)

ABSTRACT

Recent research has shown that snow cover induces extreme wintertime cooling and has detrimental impacts. Although the dramatic loss of Arctic sea ice certainly has contributed to a more extreme climate, the mechanism connecting sea-ice loss to extensive snow cover is still up for debate. In this study, a significant relationship between sea ice concentration (SIC) in the Barents-Kara (B-K) seas in November and snow cover extent over Eurasia in winter (November–January) has been found based in observational datasets and through numerical experiments. The reduction in B-K sea ice gives rise to a negative phase of Arctic Oscillation (AO), a deepened East Asia trough, and a shallow trough over Europe. These circulation anomalies lead to colder-than-normal Eurasian mid-latitude temperatures, providing favorable conditions for snowfall. In addition, two prominent cyclonic anomalies near Europe and Lake Baikal affect moisture transport and its divergence, which results in increased precipitation due to moisture advection and wind convergence. Furthermore, anomalous *E-P* flux shows that amplified upward propagating waves associated with the low SIC could contribute to the weakening of the polar vortex and southward breakouts of cold air. This work may be helpful for further understanding and predicting the snowfall conditions in the middle latitudes.

Key words: Arctic, Barents-Kara seas, sea ice, snow cover, Eurasia

Citation: Yang, Q., S. C. Kang, H. P. Yu, and Y. X. Yang, 2023: Impact of the shrinkage of Arctic Sea Ice on Eurasian snow cover changes in 1979–2021. *Adv. Atmos. Sci.*, **40**(12), 2183–2194, https://doi.org/10.1007/s00376-023-2272-x.

Article Highlights:

- Declines in November sea ice in the Barents-Kara seas are vital for variations in the snow cover extent over Eurasia in winter.
- Anomalous tropospheric and stratospheric circulations, as well as moisture flow and convergence, substantially impact the snow cover across Eurasia.

1. Introduction

Snowfall can modulate the physical properties of the Earth's surface by changing the albedo over a short time, which is well-known as a climate change indicator (King et al., 2008). Snowfall accumulates to form snow cover, which can influence other components of the earth system at various scales (Frei et al., 2012). According to Yang et al. (2019), changes in snow cover can affect climate anomalies by redistributing the land surface energy balance, further altering air circulation and climatic anomalies at regional to global scales. For example, anomalous autumn Eurasian snow cover triggers fluctuations in the Arctic Oscillation (AO) (Gong et al., 2003; Smith et al., 2011; Gastineau et al., 2017). Moreover, snow cover can influence surface air temperature anomalies (Han and Sun, 2018), the East Asian winter monsoon (Luo and Wang, 2019), and it is connected with diverse interannual variations regarding the winter Siberian high (Sun et al., 2021). Additionally, snow cover is also a critical component of the hydrological system, acting as a reservoir to slow the penetration rate of water into the soil, regulate river discharge (You et al., 2020), and influence the hydrologic cycle (Qin et al., 2014). Also, changes in

※ This paper is a contribution to the special issue on Changing Arctic Climate and Low/Mid-latitudes Connections.

* Corresponding author: Shichang KANG
Email: shichang.kang@lzb.ac.cn

snow cover caused by long-term snow accumulation can affect ecosystems. Intraseasonal and interannual variations in snow cover substantially affect human activities (Jaagus, 1997). Consequently, it is crucial to investigate snow cover, particularly its variability.

The impact of sea ice on snow cover has become increasingly significant in previous studies. Sea ice is the primary arbiter of energy exchange between the Arctic atmosphere and the ocean (Francis et al., 2009) and can potentially be a key driver in the global climate system (McBean et al., 2005; Liu and Alexander, 2007). Sea ice loss can weaken the near-surface meridional temperature gradient (Cohen et al., 2014), moisten the planetary boundary layer (Liu et al., 2012; Kim et al., 2014), and decrease the near-surface static stability (Jaiser et al., 2012). A growing body of observational data, modeling efforts, and theoretical evidence demonstrates that amplified Arctic warming and sea-ice loss have had a significant impact on the extensive snow cover and severe winters in Eurasian midlatitudes (Curry et al., 1995; Honda et al., 2009; Wang and Chen, 2010; Liu et al., 2012; Cohen et al., 2013, 2014; Zhang et al., 2019), and it is often accompanied by a negative phase of the AO/North Atlantic Oscillation (NAO) (Ogi et al., 2003; Cohen et al., 2013; Kim et al., 2014; Santolaria-Otín et al., 2020). Arctic sea ice loss can affect tropospheric circulations and systems, such as the jet stream (Rex, 1950; Cohen et al., 2013, 2014; Kidston et al., 2015), the development of the Eurasian troughs (Honda et al., 2009; Cohen et al., 2014), the Siberian high (Inoue et al., 2012; Handorf et al., 2015), the East Asia trough (Gong et al., 2001; Xu et al., 2021), and the anomalous ridge over the Ural Mountains (Zhang et al., 2018, 2019). All of the above factors favor cold continental temperatures and heavy snowfall over Eurasia. In addition to the impacts on winter climate over Eurasia, several studies also have indicated that Arctic sea ice anomalies can significantly impact the Eurasian climate in boreal spring (Chen and Wu, 2018; Chen et al., 2019; Zhang et al., 2019). Furthermore, Arctic sea ice anomalies are suggested to have a notable impact on the ENSO, the dominant air-sea coupling system in the tropics (Chen et al., 2020). Additionally, winter Arctic sea ice anomalies can generate an immediate, local, and direct atmospheric response triggered by a local enhancement of turbulent heat fluxes over the Arctic, which can alter the baroclinicity and force upward propagating waves into the stratosphere (Kim et al., 2014; Sun et al., 2015; Nakamura et al., 2016; Wu and Smith, 2016; Zhang et al., 2018). This interaction can ultimately change the geopotential height over the Arctic, reduce the westerly jet in the stratosphere, and weaken the polar vortex (Kim et al., 2014; Zhang et al., 2018). The stratospheric circulation responses are likely to persist for a couple of months, accompanied by the downward migration back to the troposphere and the surface (Sun et al., 2015; Nakamura et al., 2016). Thus, it is crucial to analyze the contribution of the declining sea ice to the interaction between the troposphere and stratosphere and the resulting climate anomalies over the Eurasian midlatitudes. Even though several investigations have explored the effects of Arctic sea ice on snow cover over Eurasia from a general circulation perspective, most of these studies have not addressed the water vapor transport component in great depth. This study investigates the relationship between Arctic sea ice and snow cover over Eurasia, discusses the mechanisms that alter the atmospheric circulation from the perspective of interactions between the troposphere and the stratosphere, and also considers variations in water vapor transport.

The remainder of this paper is organized as follows. Section 2 describes the data methodology, section 3 present the results, and section 4 provides a conclusion and final discussions.

2. Methodology

Monthly SIC and sea surface temperature (SST) are derived from the Hadley Centre Sea Ice and Sea Surface Temperature (HadISST) data set (Rayner et al., 2003) from 1979–2021. The monthly snow cover extent data is collected from the Northern Hemisphere Equal-Area Scalable Earth Grid 2.0 snow cover data set from Rutgers University (Robinson et al., 2012), representing the percentage of snow-covered days in a given month. Combined with the previous study (Robinson and Frei, 2000) and the snow cover extent anomaly and its variance (figures not shown), the snow accumulation season begins in October and November, whereas spring ablation typically occurs in March. Accordingly, snow cover from November to January of the following year is chosen as winter snow cover for the study, and an empirical orthogonal function (EOF) analysis is conducted to identify the major modes of the Eurasian snow cover. We also use globally monthly atmospheric reanalysis data from the National Centers for Environmental Prediction–National Center for Atmospheric Research reanalysis dataset, which includes the specific humidity, horizontal winds, sea level pressure (SLP), geopotential height, and air temperature, with a horizontal resolution of 2.5° × 2.5° and 17 vertical pressure levels (Kalnay et al., 1996). The observational analysis is executed after removing the linear trends, and a two-tailed Student's *t*-test is used to determine the statistical significance.

Version 5 of the National Center for Atmospheric Research Community Atmospheric Model (CAM5.0), which has a finite-volume dynamical core, is used to conduct the simulations. The simulations presented in this paper are performed at a horizontal resolution of 1.9° × 2.5° (lat. × long.). There are 30 uneven levels in the vertical direction.

To diagnose the moisture transport, we calculate the vertically integrated moisture flux. It can be expressed as:

$$\boldsymbol{Q}=\frac{1}{g}\int_{p_s}^{p_t}(q\boldsymbol{V})\,\mathrm{d}p\,. \tag{1}$$

The divergence of water vapor flux can be divided into two parts (Huang et al., 1998): the moisture advection term and the wind divergence term:

$$\nabla \cdot \boldsymbol{Q} = \frac{1}{g}\int_{p_s}^{p_t} \nabla \cdot (\boldsymbol{V}q)\,\mathrm{d}p = \frac{1}{g}\int_{p_s}^{p_t} \boldsymbol{V} \cdot \nabla q\,\mathrm{d}p + \frac{1}{g}\int_{p_s}^{p_t} q \cdot (\nabla \cdot \boldsymbol{V})\mathrm{d}p\,, \quad (2)$$

where $\boldsymbol{V}$ is the horizontal wind vector, q is the specific humidity, and p_t and p_s are defined as 300 hPa and the surface pressure, respectively. The first term on the right side indicates the moisture advection. When the wind blows from an area of high specific humidity area to a low specific humidity area, the moisture advection is negative and represents the wet advection. The second term on the right is the wind divergence term, which corresponds to divergence in the water vapor transport field.

To assess the influence of wave activity on the polar vortex and the jet, the quasi-geostrophic version of the *E-P* flux and its divergence is calculated as follows (Edmon et al., 1980):

$$\boldsymbol{F} = (F(y), F(p)) = \left[a\cos\phi\overline{u'v'}, f a\cos\phi\frac{\overline{v'\theta'}}{\theta_p}\right], \quad (3)$$

$$\nabla \cdot \boldsymbol{F} = \frac{\partial F(y)}{\partial y} + \frac{\partial F(x)}{\partial x}\,, \quad (4)$$

where ϕ is latitude, p is pressure, θ is potential temperature, a is the Earth's radius, f is the Coriolis parameter, bars and primes denote zonal means and deviations, and (u, v) is the horizontal velocity.

3. Results

3.1. *The leading mode of snow cover over Eurasia in winter*

EOF analysis is applied to the winter averaged snow cover to detect the leading mode of snow cover in Eurasia (20°–80°N, 0°–180°E). The first EOF mode (EOF1) explains about 16.8% of the total variance, approximately depicted as a west-middle-east tri-pole pattern (Fig. 1a), which exhibits a pronounced anomaly over the entirety of Europe and East Asia. The second EOF mode (EOF2) accounts for approximately 11.1% of the variance and is characterized by a "west-east" pattern (Fig. 1b). Both the first prin-

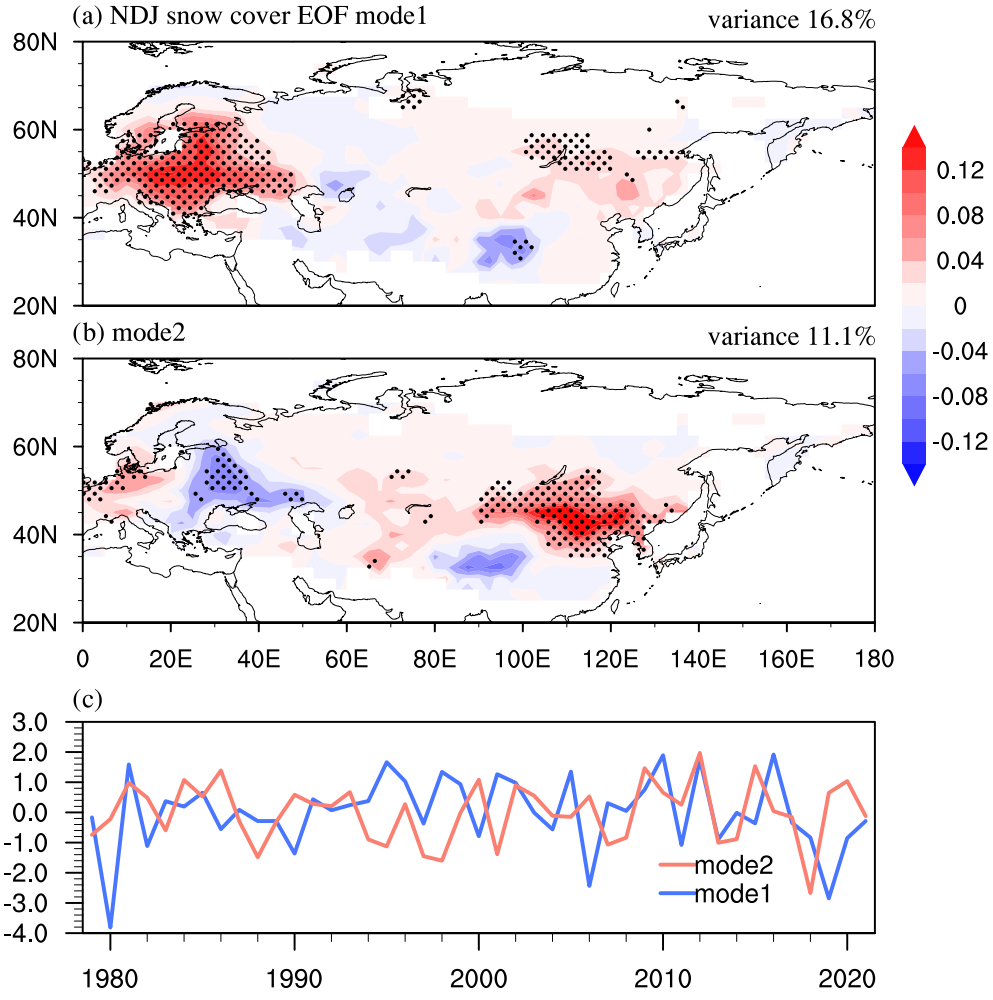

Fig. 1. (a and b) Spatial pattern and (c) corresponding principal component (blue: PC1, red: PC2) of the first and second EOF modes of normalized winter mean snow cover extent in Eurasia in 1979–2021. Values significant at the 90% confidence level are dotted.

cipal component (PC1) and the second principal component (PC2) series show remarkable interannual fluctuations (Fig. 1c). According to North et al. (1982), the first mode is independent and can be distinguished from others. Thus, we select EOF1 to study the interannual variation of winter snow cover. To investigate its possible relationship with Arctic sea ice, the correlation between the September-November Arctic SIC and the PC1 is analyzed (Figs. 2a–c). Winter snow cover is negatively correlated with the September SIC, which is widely scattered across the Pacific Ocean region (Fig. 2a). Snow cover is negatively correlated with the October SIC, which is confined to a quite small region over the B-K seas and not significant (Fig. 2b). However, the correlation is significant and negative over the B-K seas in November (Fig. 2c), which is very similar to the November sea ice over the B-K seas having the greatest influence on the middle latitudes (Koenigk et al., 2016). The relationship between snow cover and the SIC in December and January is also checked, but its signal is not as obvious as in November (Fig. S1 in the Electronic Supplementary Material, ESM). Therefore, we select the area bounded by 40°–100°E and 67°–84°N as the key region to calculate the regionally averaged November SIC and define its normalization as the B-K sea ice index (SICI).

Subsequent calculations take a negative sign for SICI (Fig. 2d). The correlation coefficient between the November Arctic SICI and the PC1 of winter snow cover is about 0.3, which is significant at the 90% confidence level. Figure 2e depicts the regression of snow cover to SICI, which closely resembles the EOF1 (Fig. 1a), illustrating that the November SIC over B-K seas correlates considerably well with the winter snow cover. A significant correlation also exists over the East Siberian Sea (ES sea). We select a key region bounded by 130°–160°E and 72°–77°N to define the ES sea ice index (ESICI), and the snow cover has been regressed to the ESICI (Fig. S2 in the ESM). The distribution of the significant snow cover is scattered in Fig. S2 and cannot be depicted by a west-middle-east triple pattern (Figs. 1a and 2e). From this, we conclude that sea-ice variability in the B-K sea in November is relative to the EOF1, which implies more extensive snow cover across Europe, Central Asia, and East Asia.

3.2. *Possible physical mechanisms for influencing of B-K SIC on snow cover*

To clarify a possible physical mechanism explaining the impact of sea ice on Eurasian snow cover, we use regression plots (Fig. 3) to analyze changes in atmospheric circulation. The resulting SLP pattern (Fig. 3a) appears zonally symmetric and resembles the typical pattern of the negative AO, which promotes Arctic cold air outbreaks in the middle latitudes (Cohen et al., 2007). While the Siberian high experiences no obvious change compared with its climatology, which differs from some previous studies (Zhang et al., 2019). This may be because the connection between the Arctic SIC and the intensity of the Siberian high is unstable. Based on Chen et al. (2021), the connection of the Arctic SIC anomalies with the winter Siberian high intensity has undergone a pronounced interdecadal change around the late-1990s. They pointed out that the SIC of the B-K seas had a significant negative correlation with the intensity of the following winter's Siberian high before the 1990s. However, the correlation after the mid-to-late-1990s decreased sharply and became statistically insignificant. Additionally, changes in the Aleutian low related to SIC were also insignificant. Based on Chen and Kang (2006), abnormal planetary wave activity is a contributing factor in regulating the intensity of the Siberian high and Aleutian low. To verify the changes of the Siberian High and Aleutian Low, we calculate wavenumber 2 for the SLP. The regression field shows that neither the Siberian High nor the Aleutian Low has changed significantly

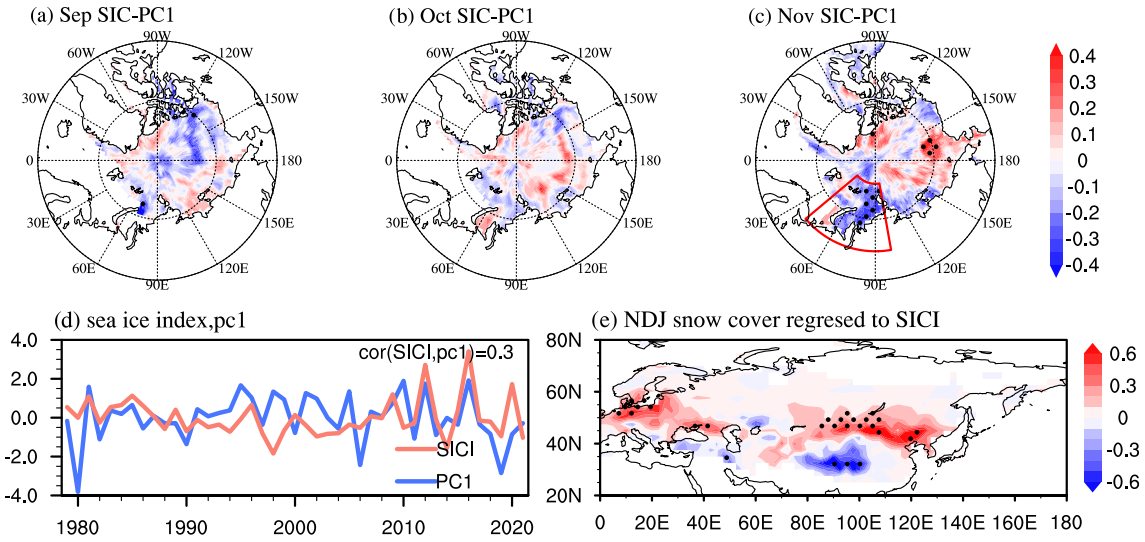

Fig. 2. Correlation maps of (a) September, (b) October, and (c) November Arctic SIC with PC1 of snow cover, respectively. The rectangle in (c) indicates the Barents-Kara Seas (40°–100°E, 67°–84°N) used to define the SICI index. (d) The series of SICI and PC1. (e) Linear regression of NDJ-mean snow cover anomalies onto the SICI. Values significant at the 90% confidence level are dotted.

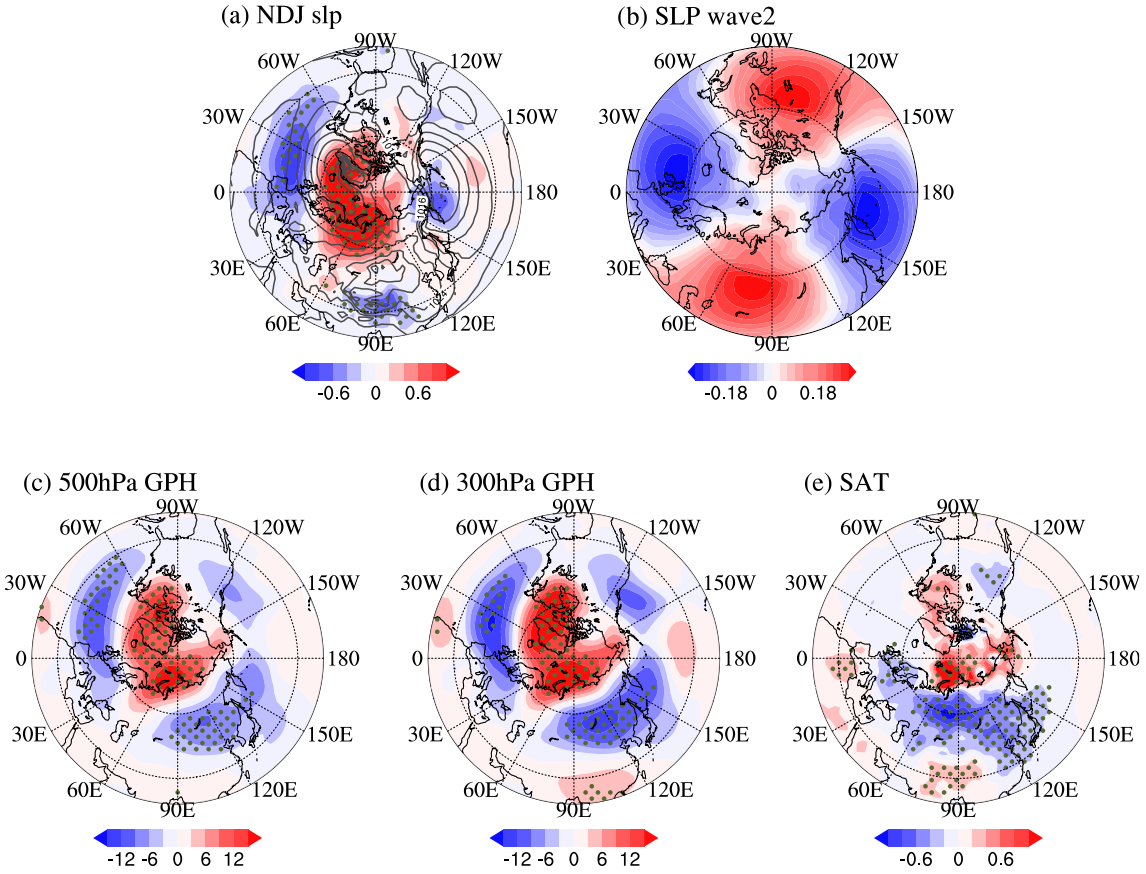

Fig. 3. Linear regressions of NDJ-mean (a) SLP (units: hPa, gray lines denote the climatological winter SLP), (b) SLP fields at wavenumber 2 (units: hPa), (c) 500-hPa geopotential height (units: m) and (d) 300-hPa geopotential height (units: m), (e) surface air temperature (SAT, units: °C) onto SICI during 1979–2021. Values significant at the 90% confidence levels are dotted.

(Fig. 3b), which is consistent with Fig. 3a. In addition, the winter geopotential height at 500 hPa (Fig. 3c) and 300 hPa (Fig. 3d) illustrates that, due to the declining sea ice, the East Asian trough and the shallow trough over Europe intensified, strengthening the cold air outbreak events and decreasing the temperature over Eurasia (Fig. 3e). This is consistent with previous studies showing that a negative AO is favorable for a deepened East Asia trough (Gong et al., 2001).

Abundant water vapor transport is also a necessary condition for snowfall; hence, changes in water vapor transport and its corresponding circulation are examined at 700 hPa where water vapor tends to be concentrated (Fig. 4). Two anomalous cyclones are located near Europe and Lake Baikal, influencing the moisture budget, which is quite compatible with the vertically integrated moisture flux according to Eq. (1), as shown in Fig. 5a. The relative contribution of the moisture advection term and the wind divergence term to water vapor convergence varies over Eurasia; therefore, a detailed analysis is considered based on Eq. (2). Winds converge on the southwestern side of Lake Baikal, increasing the water vapor convergence there (Fig. 5b), which is favorable for anomalous precipitation; while the moisture advection term mainly affects the area south of Lake Baikal and most of Europe (Fig. 5c). Thus, in Asia, the water vapor budget is influenced by the combined effect of moisture advection and wind divergence terms, whereas in Europe, the moisture advection term is more dominant. To further verify the correspondence between the water vapor budget and precipitation anomalies, we analyzed the spatial distribution of precipitable water, which represents the total amount of water vapor in the tropospheric air column. Figure 5d indicates that the precipitable water well corresponds with the large snowfall area (the slashed area), especially over East Asia. This result implies that the two cyclones near Europe and Lake Baikal play a significant role in regulating water vapor from the North Atlantic and Northwest Pacific.

Previous studies have demonstrated that the atmospheric wave activities of the stratosphere and the troposphere influence each other, especially in winter. The anomalous planetary waves, which form in the troposphere due to the declining sea ice, can propagate upward and subsequently affect the polar vortex. We investigate the energy propagation of stationary Rossby waves according to Eq. (3). To explore the difference with precision, we separate the *E-P* flux between years with high and low sea ice by one standard deviation. Figure 6a depicts the difference in *E-P* flux and its divergence between low and high SIC years. Reduced sea ice is connected with the enhanced vertical component of *E-*

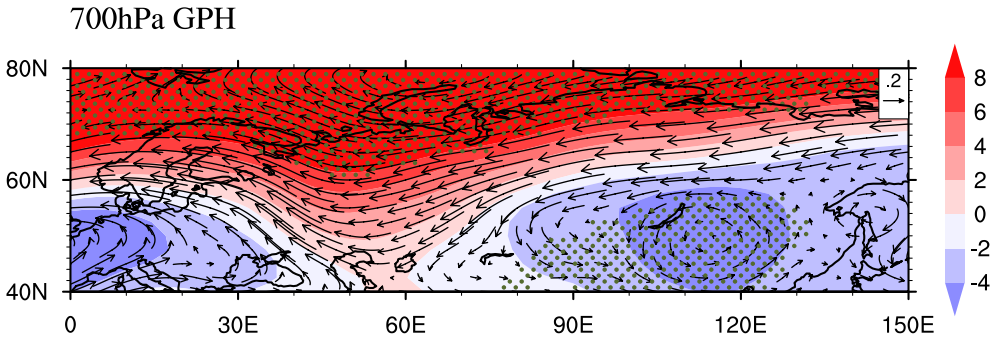

Fig. 4. Linear regressions of NDJ-mean 700-hPa wind (units: m s^{-1}) and geopotential height (units: m) onto SICI during 1979–2021. Values significant at the 90% confidence level are shown as green dots.

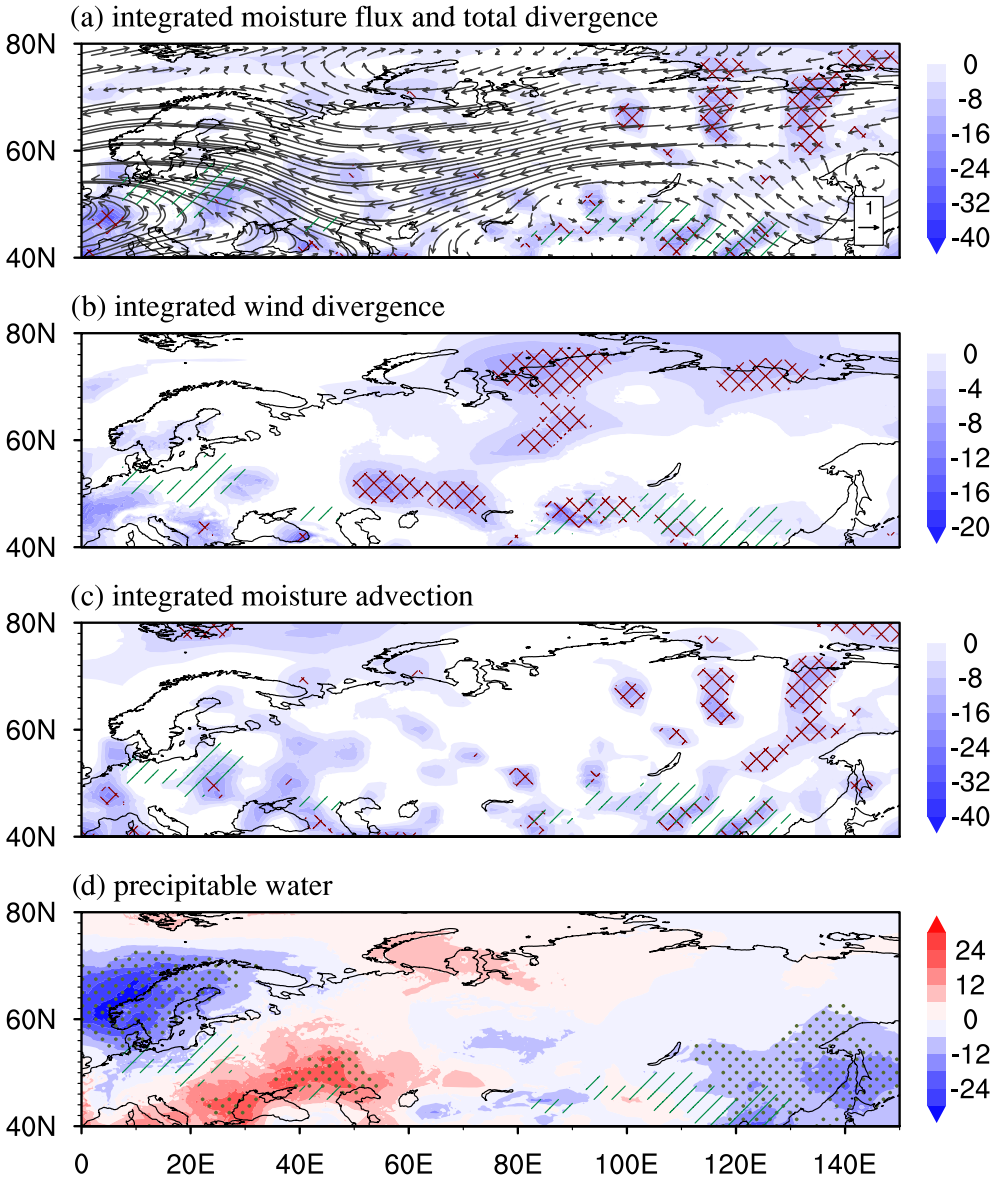

Fig. 5. Linear regressions of NDJ-mean (a) vertically integrated moisture fluxes (vector, units: kg m^{-1} s^{-1}) and their convergence (shading, units: 10^{-7} kg m^{-2} s^{-1}), (b) wind divergence term (units: 10^{-7} kg m^{-2} s^{-1}), (c) moisture advection (10^{-6} kg m^{-2} s^{-1}), (d) precipitable water (units: mm) onto SICI during 1979–2021. Crossed areas denote values exceeding the 90% confidence level, and the slashed area represents the region in Fig. 2e where the regression coefficient is greater than 0.2.

P flux in the entire troposphere north of 60°N and stratosphere north of 50°N. Consequently, the *E-P* flux near the tropopause is more obviously directed upward near the polar regions, leading to anomalous convergence of the *E-P* flux in the stratosphere. In addition, the *E-P* flux convergence is strengthened at about 40°–60°N and centered at 300 hPa, which corresponds well to the mean position of the winter polar front jet. Under such a circulation change, the intensified meridional activities will cause atmospheric blocking to become more prevalent (Rex, 1950). In conclusion, the enhanced upward propagating planetary-scale waves could penetrate the stratosphere, increase the geopotential height, decelerate the westerly jet (Fig. 6b), and weaken the stratospheric polar vortex (Fig. 6b). This pattern demonstrates that cold air in the Arctic can easily escape to the middle latitudes. To better comprehend the stratosphere–troposphere coupling to the declining sea ice, we present the response of zonal wave-1 geopotential height in Fig. 6c. The planetary wave response is in phase with the upward propagating climatological wave-1 pattern, thus when SIC is low in B-K seas, the upward wave propagation into the stratosphere becomes stronger, ultimately favoring a weaker polar vortex.

3.3. *Numerical experiments*

The statistical analysis described above implies that there are pronounced snow cover anomalies across Europe, Central, and East Asia from November to January in recent years, which may be attributed to sea-ice loss in the B-K seas, as measured in November. To support our findings, two climate model experiments using CAM5.0 are conducted. For the simulations, the SIC and SST are characterized as boundary conditions based on the Hadley Centre data sets. The control run is forced by the monthly climatological SIC and SST for the study period. To avoid physical inconsistency between the SST and SIC, the sensitivity experiment is driven by the altered SIC and SST, which are identical to the control run except for November in the B-K seas. The SIC and SST in November in the B-K seas are set as the value during the low SIC years, as defined by one standard deviation. The SIC and SST distribution in the control run and sensitivity experiment is shown in supplementary figures (Figs. S3, S4 in the ESM). Two sets of experiments were both integrated from 1 January for 40 years, and we analyzed the last 35 years. To obtain faithful atmospheric circulation responses to sea-ice loss (Screen et al., 2013; Mori et al., 2014), each experiment consists of 40 ensemble members with slightly different initial temperature perturbations.

Although some differences can be identified, the model successfully reproduces the overall response of the atmospheric circulation (Fig. 7) to the anomalously low SIC over the B-K seas. The resultant SLP pattern (Fig. 7a) shows a negative AO pattern and increased Arctic outbreaks into the middle latitudes. Meanwhile, the strength of the negative AO is stronger in the experiment, which may be caused by the higher polar amplification in the climate models (Holland and Bitz, 2003). The model successfully replicates the response of the middle and upper tropospheric circulation to the anomalously low SIC in November over the B-K seas (Figs. 7b, c). The resulting geopotential height anomaly then favors cold anomalies throughout Eurasia in winter (Fig. 7d). The difference in the distribution of SAT may come from the uncertainty of the model. There are two promi-

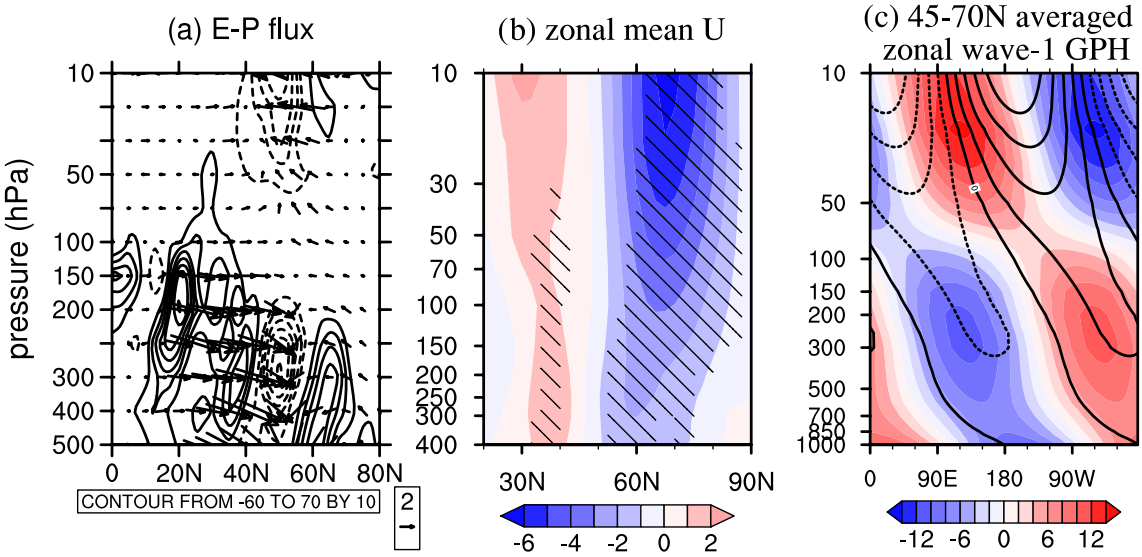

Fig. 6. (a) Difference in winter *E-P* flux (vectors, units: $m^3\ s^{-2}$) and its divergence (contours, dashed lines indicate negative values, units: $m^2\ s^{-2}$) between years with low and high SIC. (b) Same as in (a), but for zonal mean zonal wind in winter (units: $m\ s^{-1}$), hatched areas denote that the difference is significant at the 90% confidence level. (c) Same as in (a), but for the 45°–70°N averaged zonal wave-1 geopotential height (units: m) in winter. Contours denote the climatological value. Both components of *E-P* flux are multiplied by cos Φ and the square root of (1000/*p*), where Φ is the latitude, and *p* is pressure. The meridional component is divided by πa, where *a* is the Earth's radius, and the vertical component is divided by 10^5.

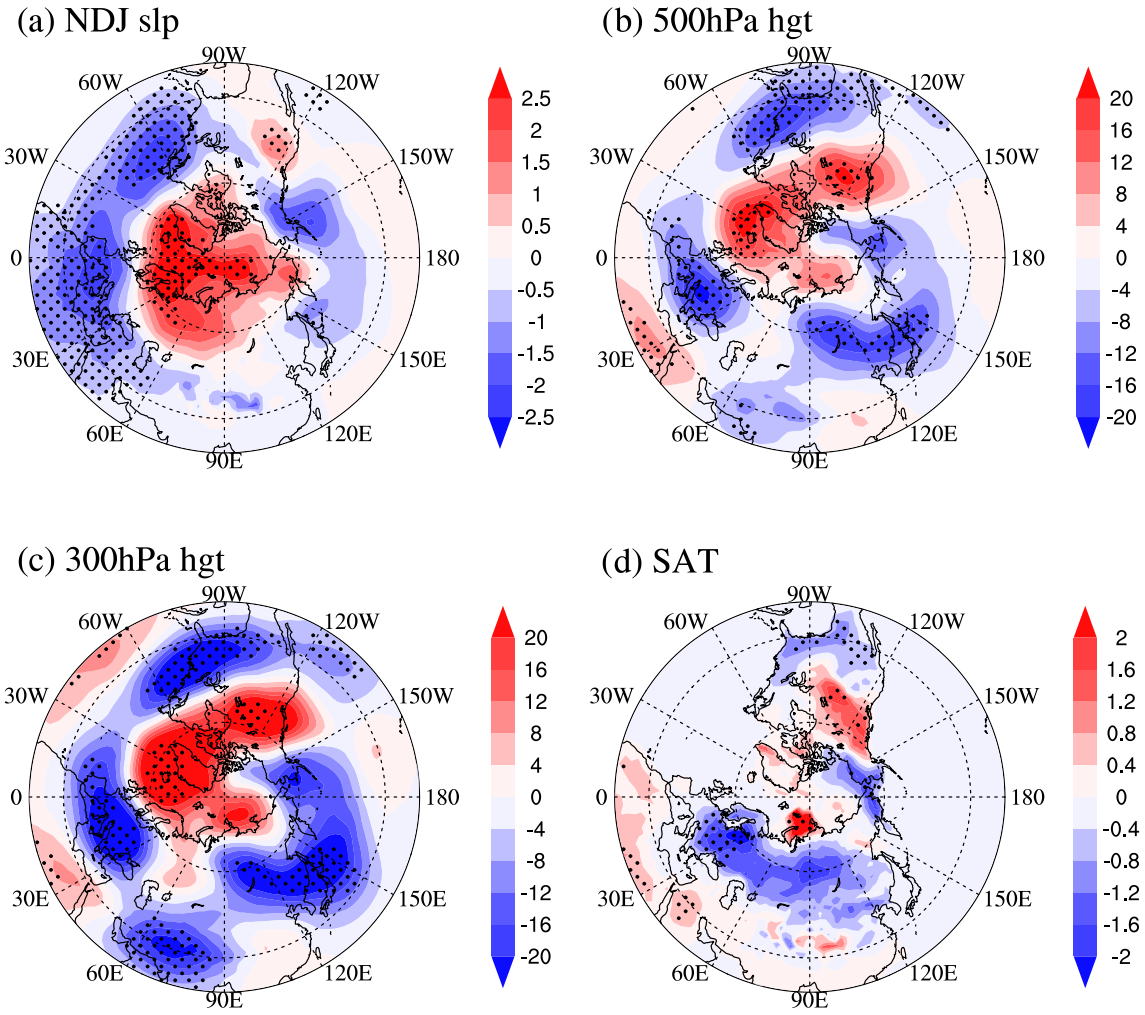

Fig. 7. Same as in Figs. 3a–d, but for the difference between the sensitivity experiment and control run in CAM5.0.

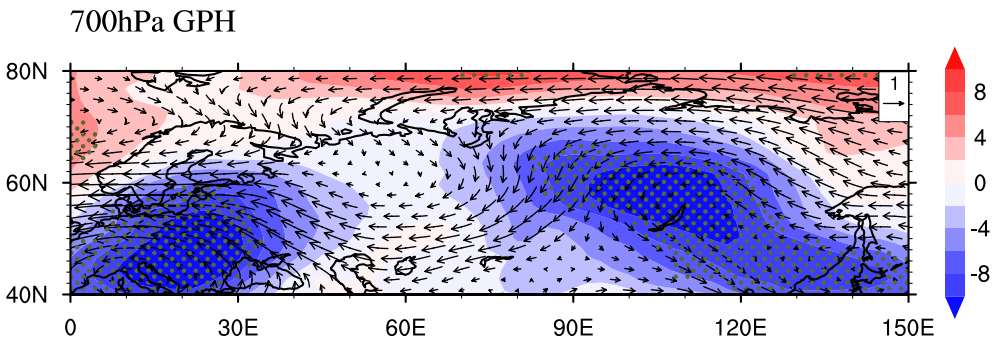

Fig. 8. Same as in Fig. 4, but for the difference between the sensitivity experiment and control run in CAM5.0.

nent cyclonic anomalies at 700 hPa in Eurasia that are consistent with the observation and favor snowfall (Fig. 8). Moreover, the quasi-stationary planetary waves propagate upward when sea ice is low in the B-K sea (Fig. 9a). These findings suggest that sea-ice loss over the B-K seas generally induces a weaker stratospheric polar vortex and westerly jet (Fig. 9b).

Consequently, there is substantial observational and modeling evidence that declining sea ice, accompanied by a negative AO, a deepened East Asia trough, and trough over Europe, and a weakened stratospheric polar vortex would result in colder Eurasian temperatures. Additionally, two prominent cyclonic anomalies near Europe and Lake Baikal affect moisture transport and convergence, inducing increased precipitation. In this way, the snow cover in Europe, as well as Central and East Asia, has increased.

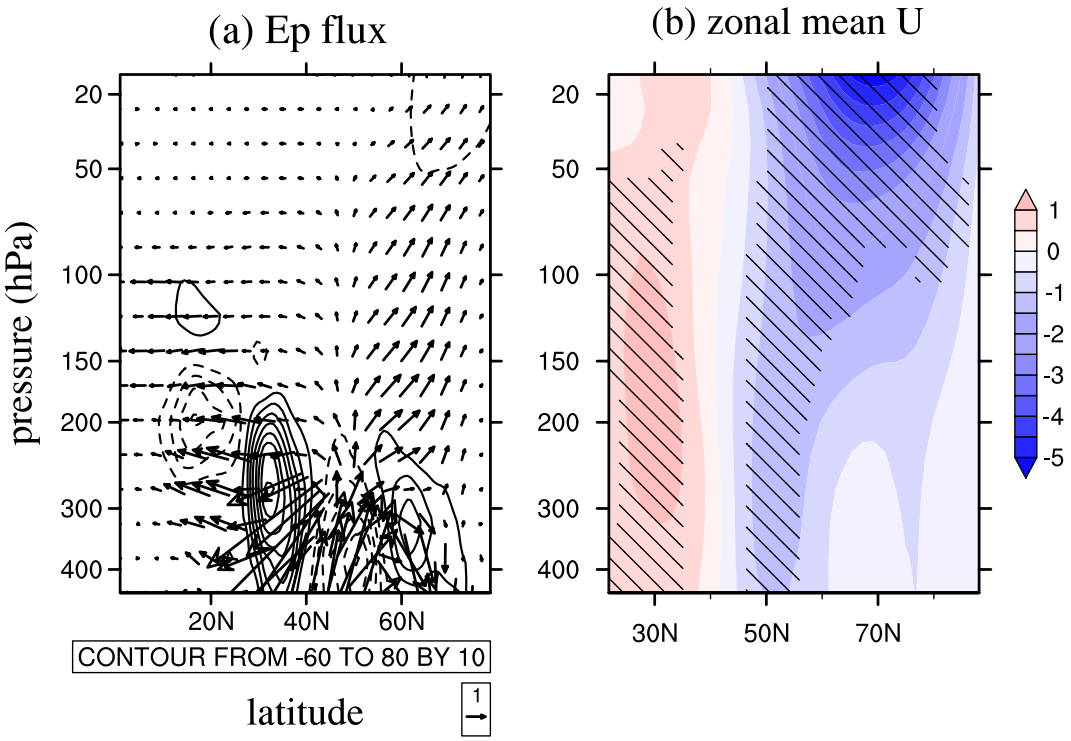

Fig. 9. Difference in (a) *E-P* flux (units: m^3 s^{-2}) and its divergence (contours, dashed lines denote negative values, units: m^2 s^{-2}), (b) zonal mean zonal wind (units: m s^{-1}) between the sensitivity experiment and control run in CAM5.0. The meridional and vertical components of the *E-P* flux are divided by 10^7 and 10^4 before the composites, respectively. Hatched areas in (b) denote that the difference is significant at the 90% confidence level.

4. Conclusion and discussion

In this study, the relationship between the early winter B-K sea ice anomaly and winter snow cover response in Eurasia is investigated through a combination of observations and climate modeling experiments. The results show that sea ice reduction over the B-K seas in November can lead to heavy snowfall in Europe, Central Asia, and East Asia. To investigate potential physical mechanisms for the impact of the November Arctic SIC on the winter snow cover variability over Eurasia, we examined the atmospheric circulation and moisture budget response. A schematic diagram illustrating how the changes in atmospheric conditions affect snow cover is shown in Fig. 10.

The declining B-K sea ice gives rise to a negative phase of AO in conjunction with a deepened East Asia trough and a deepened trough over Europe. These would induce southward cold air outbreaks and provide favorable conditions for snowfall. In addition, two prominent cyclonic anomalies near Europe and Lake Baikal regulate water vapor from the North Atlantic and Northwest Pacific and affect moisture transport and its divergence, resulting in higher snow efficiency over Eurasia. Further analysis suggests that both moisture advection and wind divergence influence snowfall in Asia, whereas moisture advection is more significant in Europe. Moreover, it is essential to recognize the connection between early winter sea ice and the variability of stratospheric dynamics. Wave activity analysis reveals that the upward *E-P* flux is strengthened and the polar vortex is weakened under low sea-ice conditions. The *E-P* flux convergence and meridional activity are considerably enhanced, resulting in colder mid-latitude temperatures.

Our findings suggest that the pronounced snow cover anomaly over Eurasia from November to January may be attributed to the sea ice reduction in the B-K seas in November. We ascribe the prolonged mid-latitude circulation response to both tropospheric and stratospheric mechanisms. From Fig. 2c, the ice in the ES sea also impacts the interannual variability of snow cover over Eurasia, which can be investigated in future work. Nonetheless, a proposed dynamical argument points out that the rapid advance of snow cover may lead to substantial Arctic sea ice melting (Cohen et al., 2013). A greater or more rapid snow cover extent in autumn contributes to a negative winter AO, allowing for the accurate prediction of cold winter temperatures over Eurasia (Cohen et al., 2007, 2013). Thus, further work is required to completely understand the implications of sea ice by utilizing the ocean-ice-atmosphere interaction coupled models. Moreover, this study only examines the mean thermal effects, while the feedback of the eddy on the Amplified Arctic warming is contrary to the mean flow (Sang et al., 2022). Thus, the feedback forcing between mean flows and transient

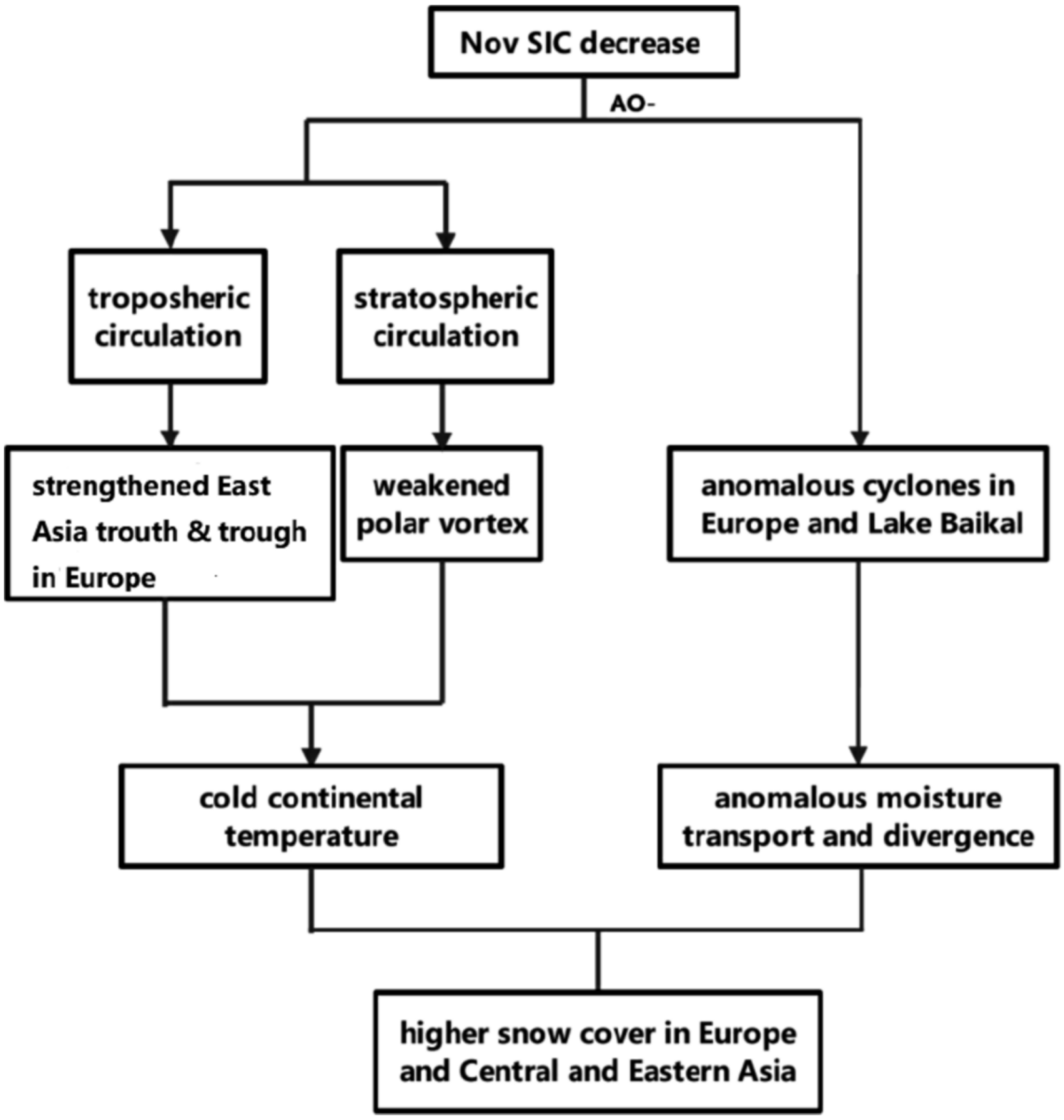

Fig. 10. A schematic diagram shows how the declining SIC affects the winter snow cover in Eurasia.

eddy activities is also worth considering.

Acknowledgements This paper was financially supported by the International Partnership Program of Chinese Academy of Sciences (Grant No. 131B62KYSB20180003), the Frontier Science Key Project of CAS (Grant No. QYZDY-SSW-DQC021), and the State Key Laboratory of Cryospheric Science (Grant No. SKLCS-ZZ-2022).

Electronic supplementary material: Supplementary material is available in the online version of this article at https://doi.org/10.1007/s00376-023-2272-x.

REFERENCES

Chen, S. F., and R. G. Wu, 2018: Impacts of early autumn Arctic sea ice concentration on subsequent spring Eurasian surface air temperature variations. *Climate Dyn.*, **51**, 2523–2542, https://doi.org/10.1007/s00382-017-4026-x.

Chen, S. F., R. G. Wu, and W. Chen, 2019: Enhanced impact of Arctic sea ice change during boreal autumn on the following spring Arctic oscillation since the mid-1990s. *Climate Dyn.*, **53**, 5607–5621, https://doi.org/10.1007/s00382-019-04886-y.

Chen, S. F., R. G. Wu, W. Chen, and B. Yu, 2020: Influence of winter Arctic sea ice concentration change on the El Niño-Southern oscillation in the following winter. *Climate Dyn.*, **54**, 741–757, https://doi.org/10.1007/s00382-019-05027-1.

Chen, S. F., R. G. Wu, W. Chen, L. Y. Song, W. Cheng, and W. J. Shi, 2021: Weakened impact of autumn Arctic sea ice concentration change on the subsequent winter Siberian high variation around the late-1990s. *International Journal of Climatology*, **41**, E2700–E2717, https://doi.org/10.1002/JOC.6875.

Chen, W., and L. H. Kang, 2006: Linkage between the Arctic oscillation and winter climate over east Asia on the interannual

timescale: Roles of quasi-stationary planetary waves. *Chinese Journal of Atmospheric Sciences*, **30**, 863–870, https://doi.org/10.3878/j.issn.1006-9895.2006.05.15. (in Chinese with English abstract)

Cohen, J., M. Barlow, P. J. Kushner, and K. Saito, 2007: Stratosphere–troposphere coupling and links with eurasian land surface variability. *J. Climate*, **20**, 5335–5343, https://doi.org/10.1175/2007JCLI1725.1.

Cohen, J., J. Jones, J. C. Furtado, and E. Tziperman, 2013: Warm Arctic, cold continents: A common pattern related to Arctic sea ice melt, snow advance, and extreme winter weather. *Oceanography*, **26**, 150–160, https://doi.org/10.5670/oceanog.2013.70.

Cohen, J., and Coauthors, 2014: Recent Arctic amplification and extreme mid-latitude weather. *Nature Geoscience*, **7**, 627–637, https://doi.org/10.1038/ngeo2234.

Curry, J. A., J. L. Schramm, and E. E. Ebert, 1995: Sea ice-albedo climate feedback mechanism. *J. Climate*, **8**, 240–247, https://doi.org/10.1175/1520-0442(1995)008<0240:SIACFM>2.0.CO;2.

Edmon, H. J. Jr., B. J. Hoskins, and M. E. Mcintyre, 1980: Eliassen-palm cross sections for the troposphere. *J. Atmos. Sci.*, **37**, 2600–2616, https://doi.org/10.1175/1520-0469(1980)037<2600:EPCSFT>2.0.CO;2.

Francis, J. A., W. Chan, D. J. Leathers, J. R. Miller, and D. E. Veron, 2009: Winter Northern Hemisphere weather patterns remember summer Arctic sea-ice extent. *Geophys. Res. Lett.*, **36**, L07503, https://doi.org/10.1029/2009GL037274.

Frei, A., M. Tedesco, S. Lee, J. Foster, D. K. Hall, R. Kelly, and D. A. Robinson, 2012: A review of global satellite-derived snow products. *Advances in Space Research*, **50**, 1007–1029, https://doi.org/10.1016/j.asr.2011.12.021.

Gastineau, G., J. García-Serrano, and C. Frankignoul, 2017: The influence of autumnal eurasian snow cover on climate and its link with Arctic sea ice cover. *J. Climate*, **30**, 7599–7619, https://doi.org/10.1175/JCLI-D-16-0623.1.

Gong, D.-Y., S.-W. Wang, and J.-H. Zhu, 2001: East Asian winter monsoon and Arctic oscillation. *Geophys. Res. Lett.*, **28**, 2073–2076, https://doi.org/10.1029/2000GL012311.

Gong, G., D. Entekhabi, and J. Cohen, 2003: Modeled Northern Hemisphere winter climate response to realistic siberian snow anomalies. *J. Climate*, **16**, 3917–3931, https://doi.org/10.1175/1520-0442(2003)016<3917:MNHWCR>2.0.CO;2.

Han, S. Z., and J. Q. Sun, 2018: Impacts of autumnal eurasian snow cover on predominant modes of boreal winter surface air temperature over eurasia. *J. Geophys. Res.: Atmos.*, **123**, 10 076–10 091, https://doi.org/10.1029/2018JD028443.

Handorf, D., R. Jaiser, K. Dethloff, A. Rinke, and J. Cohen, 2015: Impacts of Arctic sea ice and continental snow cover changes on atmospheric winter teleconnections. *Geophys. Res. Lett.*, **42**, 2367–2377, https://doi.org/10.1002/2015GL063203.

Holland, M. M., and C. M. Bitz, 2003: Polar amplification of climate change in coupled models. *Climate Dyn.*, **21**, 221–232, https://doi.org/10.1007/s00382-003-0332-6.

Honda, M., J. Inoue, and S. Yamane, 2009: Influence of low Arctic sea-ice minima on anomalously cold Eurasian winters. *Geophys. Res. Lett.*, **36**, L08707, https://doi.org/10.1029/2008GL037079.

Huang, R. H., Z. Z. Zhang, G. Huang, and B. H. Ren, 1998: Characteristics of the water vapor transport in east Asian monsoon region and its difference from that in south Asian monsoon region in summer. *Chinese Journal of Atmospheric Sciences*, **22**, 460–469, https://doi.org/10.3878/j.issn.1006-9895.1998.04.08. (in Chinese with English abstract)

Inoue, J., M. E. Hori, and K. Takaya, 2012: The role of barents sea ice in the wintertime cyclone track and emergence of a warm-Arctic cold-siberian anomaly. *J. Climate*, **25**, 2561–2568, https://doi.org/10.1175/JCLI-D-11-00449.1.

Jaagus, J., 1997: The impact of climate change on the snow cover pattern in Estonia. *Climatic Change*, **36**, 65–77, https://doi.org/10.1023/A:1005304720412.

Jaiser, R., K. Dethloff, D. Handorf, A. Rinke, and J. Cohen, 2012: Impact of sea ice cover changes on the Northern Hemisphere atmospheric winter circulation. *Tellus A: Dynamic Meteorology and Oceanography*, **64**, 11595, https://doi.org/10.3402/tellusa.v64i0.11595.

Kalnay, E., and Coauthors, 1996: The NCEP/NCAR 40-year reanalysis project. *Bull. Amer. Meteor. Soc.*, **77**, 437–472, https://doi.org/10.1175/1520-0477(1996)077<0437:TNYRP>2.0.CO;2.

Kidston, J., A. A. Scaife, S. C. Hardiman, D. M. Mitchell, N. Butchart, M. P. Baldwin, and L. J. Gray, 2015: Stratospheric influence on tropospheric jet streams, storm tracks and surface weather. *Nature Geoscience*, **8**, 433–440, https://doi.org/10.1038/ngeo2424.

Kim, B.-M., S.-W. Son, S.-K. Min, J.-H. Jeong, S.-J. Kim, X. D. Zhang, T. Shim, and J.-H. Yoon, 2014: Weakening of the stratospheric polar vortex by Arctic sea-ice loss. *Nature Communications*, **5**, 4646, https://doi.org/10.1038/ncomms5646.

King, J. C., and Coauthors, 2008: Snow-atmosphere energy and mass balance. *Snow and Climate, Physical Processes, Surface Energy Exchange and Modelling*, R. Armstrong and E. Brun, Eds., Cambridge University Press, 70–124.

Koenigk, T., M. Caian, G. Nikulin, and S. Schimanke, 2016: Regional Arctic sea ice variations as predictor for winter climate conditions. *Climate Dyn.*, **46**, 317–337, https://doi.org/10.1007/s00382-015-2586-1.

Liu, J. P., J. A. Curry, H. J. Wang, M. R. Song, and R. M. Horton, 2012: Impact of declining Arctic sea ice on winter snowfall. *Proceedings of the National Academy of Sciences of the United States of America*, **109**, 4074–4079, https://doi.org/10.1073/pnas.1114910109.

Liu, Z. Y., and M. Alexander, 2007: Atmospheric bridge, oceanic tunnel, and global climatic teleconnections. *Rev. Geophys.*, **45**, RG2005, https://doi.org/10.1029/2005RG000172.

Luo, X., and B. Wang, 2019: How autumn Eurasian snow anomalies affect east asian winter monsoon: A numerical study. *Climate Dyn.*, **52**, 69–82, https://doi.org/10.1007/s00382-018-4138-y.

McBean, G., and Coauthors, 2005: Arctic climate: Past and present. *Arctic Climate Impact Assessment: Scientific Report*. ACIA, Ed., Cambridge University Press, 22–60.

Mori, M., M. Watanabe, H. Shiogama, J. Inoue, and M. Kimoto, 2014: Robust Arctic sea-ice influence on the frequent Eurasian cold winters in past decades. *Nature Geoscience*, **7**, 869–873, https://doi.org/10.1038/ngeo2277.

Nakamura, T., K. Yamazaki, K. Iwamoto, M. Honda, Y. Miyoshi, Y. Ogawa, Y. Tomikawa, and J. Ukita, 2016: The stratospheric pathway for Arctic impacts on midlatitude climate. *Geophys. Res. Lett.*, **43**, 3494–3501, https://doi.org/10.1002/2016GL068330.

North, G. R., T. L. Bell, R. F. Cahalan, and F. J. Moeng, 1982: Sampling errors in the estimation of empirical orthogonal func-

tions. *Monthly Weather Review*, **110**, 699–706, https://doi.org/10.1175/1520-0493(1982)110<0699:SEITEO>2.0.CO;2.

Ogi, M., Y. Tachibana, and K. Yamazaki, 2003: Impact of the wintertime north Atlantic oscillation (NAO) on the summertime atmospheric circulation. *Geophys. Res. Lett.*, **30**, 1704, https://doi.org/10.1029/2003GL017280.

Qin, D. H., B. T. Zhou, and C. D. Xiao, 2014: Progress in studies of cryospheric changes and their impacts on climate of China. *J. Meteor.Res.*, **28**, 732–746, https://doi.org/10.1007/s13351-014-4029-z.

Rayner, N. A., D. E. Parker, E. B. Horton, C. K. Folland, L. V. Alexander, D. P. Rowell, E. C. Kent, and A. Kaplan, 2003: Global analyses of sea surface temperature, sea ice, and night marine air temperature since the late nineteenth century. *J. Geophys. Res.: Atmos.*, **108**, 4407, https://doi.org/10.1029/2002JD002670.

Rex, D. F., 1950: Blocking action in the middle troposphere and its effect upon regional climate. *Tellus*, **2**, 275–301, https://doi.org/10.3402/tellusa.v2i4.8603.

Robinson, D. A., and A. Frei, 2000: Seasonal variability of Northern Hemisphere snow extent using visible satellite data. *The Professional Geographer*, **52**, 307–315, https://doi.org/10.1111/0033-0124.00226.

Robinson, D. A., T. W. Estilow, and NOAA CDR Program, 2012: NOAA climate data record (CDR) of Northern Hemisphere (NH) snow cover extent (SCE), version 1. Available online at :[https://www.ncei.noaa.gov/access/metadata/landing-page/bin/iso?id=gov.noaa.ncdc:C00756].

Sang, X. Z., X.-Q. Yang, L. F. Tao, J. B. Fang, and X. G. Sun, 2022: Decadal changes of wintertime poleward heat and moisture transport associated with the amplified Arctic warming. *Climate Dyn.*, **58**, 137–159, https://doi.org/10.1007/S00382-021-05894-7.

Santolaria-Otín, M., J. García-Serrano, M. Ménégoz, and J. Bech, 2020: On the observed connection between Arctic sea ice and Eurasian snow in relation to the winter north Atlantic oscillation. *Environmental Research Letters*, **15**, 124010, https://doi.org/10.1088/1748-9326/abad57.

Screen, J. A., I. Simmonds, C. Deser, and R. Tomas, 2013: The atmospheric response to three decades of observed Arctic sea ice loss. *J. Climate*, **26**, 1230–1248, https://doi.org/10.1175/JCLI-D-12-00063.1.

Smith, K. L., P. J. Kushner, and J. Cohen, 2011: The role of linear interference in northern annular mode variability associated with Eurasian snow cover extent. *J. Climate*, **24**, 6185–6202, https://doi.org/10.1175/JCLI-D-11-00055.1.

Sun, C. H., J. Q. Zuo, X. H. Shi, X. W. Liu, and H. W. Liu, 2021: Diverse inter-annual variations of winter Siberian high and link with Eurasian snow in observation and BCC-CSM2-MR coupled model simulation. *Frontiers in Earth Science*, **9**, 761311, https://doi.org/10.3389/feart.2021.761311.

Sun, L. T., C. Deser, and R. A. Tomas, 2015: Mechanisms of stratospheric and tropospheric circulation response to projected Arctic sea ice loss. *J. Climate*, **28**, 7824–7845, https://doi.org/10.1175/JCLI-D-15-0169.1.

Wang, L., and W. Chen, 2010: Downward Arctic oscillation signal associated with moderate weak stratospheric polar vortex and the cold December 2009. *Geophys. Res. Lett.*, **37**, L09707, https://doi.org/10.1029/2010GL042659.

Wu, Y. T., and K. L. Smith, 2016: Response of Northern Hemisphere midlatitude circulation to Arctic amplification in a simple atmospheric general circulation model. *J. Climate*, **29**, 2041–2058, https://doi.org/10.1175/JCLI-D-15-0602.1.

Xu, M., W. S. Tian, J. K. Zhang, T. Wang, and K. Qie, 2021: Impact of sea ice reduction in the barents and kara seas on the variation of the East Asian trough in late winter. *J. Climate*, **34**, 1081–1097, https://doi.org/10.1175/JCLI-D-20-0205.1.

Yang, M. X., X. J. Wang, G. J. Pang, G. N. Wan, and Z. C. Liu, 2019: The Tibetan Plateau cryosphere: Observations and model simulations for current status and recent changes. *Earth-Science Reviews*, **190**, 353–369, https://doi.org/10.1016/j.earscirev.2018.12.018.

You, Q. L., and Coauthors, 2020: Review of snow cover variation over the Tibetan Plateau and its influence on the broad climate system. *Earth-Science Reviews*, **201**, 103043, https://doi.org/10.1016/j.earscirev.2019.103043.

Zhang, P. F., Y. T. Wu, and K. L. Smith, 2018: Prolonged effect of the stratospheric pathway in linking Barents–Kara Sea sea ice variability to the midlatitude circulation in a simplified model. *Climate Dyn.*, **50**, 527–539, https://doi.org/10.1007/s00382-017-3624-y.

Zhang, R. N., C. H. Sun, R. H. Zhang, W. J. Li, and J. Q. Zuo, 2019: Role of Eurasian snow cover in linking winter - spring Eurasian coldness to the autumn Arctic sea ice retreat. *J. Geophys. Res.: Atmos.*, **124**, 9205–9221, https://doi.org/10.1029/2019JD030339.